Hindawi
Geofluids
Volume 2021, Article ID 8866028, 8 pages
https://doi.org/10.1155/2021/8866028

Research Article

Experimental Study on the Damage and Degradation Characteristics of Red Sandstone after Dry and Wet Cycling by Low Magnetic Field Nuclear Magnetic Resonance (NMR) Technique

Yuan Zhao, Jiangteng Li, and Gang Ma

School of Resources and Safety Engineering, Central South University, Changsha, Hunan 410083, China

Correspondence should be addressed to Jiangteng Li; ljtcsu@163.com

Received 25 June 2020; Revised 23 July 2020; Accepted 19 March 2021; Published 12 April 2021

Academic Editor: Jinze Xu

To study the damage evolution of rocks under the action of wet and dry cycles, nuclear magnetic resonance (NMR) technology was used to test red sandstone under different times of wet and dry cycles. The T_2 spectral distribution curve, porosity, spectral peak area, and damage distribution curve of the rock were obtained, and the quantitative relationship between porosity, damage degree, and number of cycles was established. The results show that with the increase of the number of wet and dry cycles, the T_2 spectral curve of rock gradually moves to the right, but the moving amplitude gradually decreases. The porosity and spectral area increase with the increase of the number of wet and dry cycles, coupled with a declining growth rate, and the maximum increase in porosity is 18.789%. The damage degree of rock increase with the increase of the number of cycles, but with the continuous increase of the number of cycles, the damage rate decreases, and finally the damage degree of rock tends to be a constant value.

1. Introduction

The interaction between water and rock means that water (surface water, groundwater, and snow water) and rock and soil body continuously carry out mechanical, physical, chemical and mechanical actions, and influence the state of rock and soil medium [1]. This problem is one of the basic research subjects of geotechnical engineering (slope, dangerous rock, dam foundation, cultural relic protection, etc.) and is playing an increasingly important role in solving the environmental pollution and ecological security problems faced by human beings. Red sandstone is concentrated in southern cities with abundant precipitation in China. In practical projects, the dry and wet cycle process destroys the integrity of the rock, changes the seepage field, provides a path for water infiltration, reduces the strength of the rock, and causes engineering accidents, causing heavy losses to the country and people. Therefore, it is of great significance to study the interaction of water and rock, especially the dry and wet cycle.

At present, many scholars have carried out a series of researches on rock physical properties, crack propagation law, and seepage law under the dry-wet cycle. Lin et al. [2–4] used laboratory tests and PFC simulation experiments to study the rock joint constitutive relationship, the constitutive relationship under the tensile state of crack tip, and the quantitative analysis method based on shear stress difference; Chen [5] conducted uniaxial compression tests on the slope rocks of open pit mine under the action of different times of dry and wet cycles and obtained the internal relations among the total work of external forces, elastic energy, and energy dissipation; Fu et al. [6] carried out uniaxial compressive and splitting tests on sandstone (saturated state) after water-rock interaction and analyzed the irreversible gradual damage to sandstone caused by dry and wet cycling; Zhao et al. [7–10] carried out a variety of laboratory tests on fractured rocks and analyzed rheological fracture behavior under different single conditions or coupling conditions; Han et al. [11] carried out chemical corrosion and dry and wet cycling

of sandstone containing type I fractures and analyzed the deterioration law of physical and mechanical properties of samples with the number of dry and wet cycles; Li et al. [12], based on the uniaxial compression test results of sandstone under different dry-wet cycles, a 2-12-1 three-layer neural network constitutive model was constructed; Zhou et al. [13] introduced water influence factor through compression test of dry and saturated sandstone specimens and concluded that its value decreased with the increase of strain rate; Wang et al. [14–16] carried out a variety of laboratory tests on rock-soil specimens with defects, studied the mechanism of crack initiation with a variety of parameters, and studied the fracture characteristics of granite under impact load; according to the adsorption isotherm, Li [17] can calculate the characteristics of pore volume and pore diameter distribution and divide the average pore diameter of tight sandstone into micropore (<10 nm), mesopore (10-50 nm), and macropore (>50 nm); Yan et al. [18] studied ten types of typical rocks in China and divided the pore size of granite into three categories: micropore (<0.01 μm), mesopore (0.01~1 μm), and macropore (≥1 μm).

The continuous improvement of the accuracy of modern observation instruments has promoted the development of rocks from macroscopic to microscopic. Specifically, the research and development of low-field NMR technology has enriched the means of rock microscopic study. Porosity, pore size distribution, water content, and other parameters related to pore structure can be obtained through it, and its detection results are characterized by quantification, which has unique advantages in the identification of pore structure change and damage evolution. In recent years, Frosch et al. [19] proved that NMR method is a noninvasive method for analyzing undisturbed reservoir sandstones with original fluid content; Zhou et al. [20] used nuclear magnetic resonance technology to conduct measurement tests on granite to provide a basis for studying the damage mechanism of rock; Li et al. [21] analyzed the relationship between NMR porosity and spectral area of freeze-thawed granite and uniaxial compressive strength by using nuclear magnetic resonance system; Sun et al. [22] took granite samples from the high-level waste disposal repository in Beishan, Gansu Province, China, as the research object and used the low-field nuclear magnetic resonance system to carry out laboratory experiments on the thermal stability of the granite at the key pre-selected sites; Ren et al. [23] carried out cyclic loading and unloading tests on water-saturated sandstone under laboratory conditions and combined acoustic emission technology and nuclear magnetic resonance analysis technology to explore the evolution law of its macro-and microdeformation and fatigue damage.

However, with the development of science and technology and the exploration of unknown areas, scholars pay more and more attention to the damage research of water-rock interaction (freeze-thaw and dry-wet). The study of rock is mostly carried out by traditional methods and stays at the macroscopic level. Therefore, in this paper, a new nondestructive testing method (NMR technology) was used to detect red sandstone with different wetting and drying cycles and analyze its meso-damage and deterioration characteristics, which provided a theoretical basis for the stability of sandstone under the action of water and rock in the future.

2. Geological History

The area of Chuxiong County in Yunnan Province is mountainous, and the mountainous area accounts for more than 90% of the total area of the whole state. It is a region dominated by high mountains and low hills, which is known as "nine points of mountains and rivers and one point of DAMS." The climate of Chuxiong Prefecture is a subtropical monsoon climate, the rainy season is from July to October, and it is located in an area with high sunshine value in Yunnan Province. The bedrock in the territory is mainly exposed in the Lower Paleozoic Ailaoshan Group, Mesozoic and Cenozoic strata, and the Triassic, Jurassic, and Cretaceous strata are widely distributed, which are mainly sandstone, argillaceous sandstone, mudstone, and marl [24].

Yunnan red sandstone refers to the red strata formed in Western Europe during the Permian to Triassic Period, consisting of red, green, and purple sandstones, arkose, and shales, marking a kind of desert deposition in dry climate conditions, with marine interlayers.

3. Experimental Materials and Methods

3.1. Experimental Materials. Red sandstone samples were extracted from Wuding County, Chuxiong Yi Autonomous Prefecture, Yunnan Province, and processed into Φ50mm $\times$ 100 mm standard cylinder specimen as per the requirements of engineering rock test regulations. To reduce the influence of discreteness, all samples were taken from the same rock mass. The machining accuracy of the specimen requires that the nonparallelism error of the two end faces $\leq$ 0.05 mm, and the diameter error $\leq$ 0.25°.

3.2. Experimental Methods. 5 groups of sandstone were selected for 0, 1, 3, 6, and 10 dry and wet cycles, with 3 specimens in each group, and adopted natural soaking method for dry and wet cycles, that is, according to the rock test rules of water conservancy and hydropower projects: the solution is added to 1/4 of the sandstone sample height for the first time and then to 1/2 and 3/4 of the sample every 2 hours. After 6 hours, all sandstone samples were immersed in the solution, and the final solution height exceeded 5 cm on the sandstone sample surface. Specific operation procedure: the rock samples were dried in an oven at 105°C for 12 hours; after it is cooled to room temperature, it is saturated with free water (distilled water) for 48 h, which is a dry and wet cycle. Repeat the above operation to 10 cycles; after the end of the cycle, we carried out the NMR experiment by wrapping the rock sample with plastic wrap (to eliminate the influence of water loss and wipe the excess water on the surface of the rock sample after the dry and wet cycle was completed). The test used the AnimR-150 rock magnetic resonance imaging analysis system (Figure 1) produced by Shanghai Newmai Electronics Technology limited company. After the experiment, the T_2 spectrum and porosity of each group were measured successively.

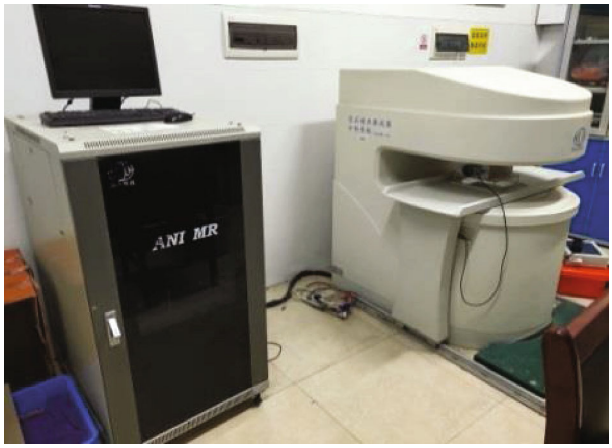

Figure 1: Rock magnetic resonance imaging of AniMR-150.

4. Analysis of Experimental Results

4.1. T_2 Spectrum Results Analysis. Nuclear magnetic resonance (NMR) was used to measure the red sandstone after different times of dry and wet cycle tests. Figure 2 shows the T_2 spectrum corresponding to different cycles of typical samples. All the T_2 spectrum curves are continuous and smooth, with three different peak spectra. From left to right, they correspond to the changes in the quantity distribution of small, medium, and large pores. It can be seen from the figure that both small and medium pores in red sandstone account for the majority, while the large pores account for less. With the increase of the number of dry and wet cycles, the height of the first peak and the second peak gradually increased, indicating that the number of dry and wet cycles increased, and the number of small and medium pores in red sandstone increased gradually. The dry and wet cycles promote the aggravation of the damage inside the rock. The heights of the third peak do not increase significantly, but it shows a trend of moving to the right, indicating that the size of the macropores is also increasing during the dry-wet cycle.

The 0-1 change curve of the dry-wet cycle is similar, and the number of small and medium pores increases slightly, among which the medium pores are relatively small, while the large pores are greatly affected by the dry-wet cycle. This shows that the first cycle has no obvious influence on the aggravation of the damage of red sandstone. After 3-10 cycles of dry and wet, the T_2 distribution spectrum increases, and the increment is more obvious than that of 0-1cycles, but the increased amplitude decreases within 3-10 cycles, and the third peak moves to the right obviously after 10 cycles, indicating that the number of large pores increases. This is because as the growth of the dry-wet cycles, the inside of the rock under the action of soluble substances in the water dissolved gradually produces new small pores, and with the increase of damage, small, medium pores development, constantly extend toward big pores, internally caused by increasing the number of pores, fractures, but the decrease of soluble substances will lead to a reduced increment of pore number, finally reaching at a constant value.

4.2. Cumulative Porosity. Porosity is the percentage of the pore volume in the total volume of the material. Porosity reflects the pore condition of the material. Figure 3 shows the variation of accumulated porosity of red sandstone with time under different cycles. Figure 3 shows that when the number of cycles is 0 and 1, the accumulated porosity-time curve of NMR basically coincides, indicating that the dry-wet cycle has little influence on the porosity in the two groups of cycles. The same is true for cycles of 3 and 6. With the increase of the number of wet and dry cycles, the porosity is gradually increased. After 0 to 10 dry and wet cycles, the porosity increases by 18.783%, and this is a significant increment.

Five dry and wet cycles were carried out in the experiment. Table 1 shows the porosity change after the dry and wet cycles. By fitting the porosity of the rock sample with the number of dry and wet cycles, the relation between porosity and the number of dry and wet cycles can be obtained, as shown in Figure 4. The fitting results can be expressed in Formula (1). The correlation coefficient is $R^2 = 0.98354$, showing a good correlation:

$$n = 10.47 - 0.7825e^{(-N/2.2424)}, \quad (1)$$

where n is the porosity of the rock sample after each dry and wet cycle, and N is the number of dry and wet cycles.

It can be seen from Figures 3 and 4 that the porosity of rock samples increases rapidly during 0-3 cycles, but increase at a lower rate during 3-6 cycles, and tends to be flat during 6-10 cycles. The reasons are as follows: at the beginning of the cycle, soluble minerals and cements inside the rock are continuously dissolved by water during the cycle, resulting in the conversion of the original closed pores into open pores. Meanwhile, the pores are also subjected to the pressure of water, resulting in the continuous expansion and penetration of the pore size. With the increase of the number of cycles, the content of soluble mineral and cement in the pore decreases, which leads to the decrease of the pore growth rate. During the cycling process, the reason for the decrease of porosity is that under the continuous action of the dry-wet cycle, a small amount of particle stripping occurs in the rock sample, resulting in a low participation quality of the rock sample and a decrease in porosity.

4.3. NMR Spectrum Area. Nuclear magnetic resonance T_2 spectrum area can reflect the change of pore size and number inside the rock, and the spectral peak area is positively correlated with the size and number of corresponding pores [25]. The characteristics of pore size distribution of rock provide an important basis for the study of permeability, pore structure, and pore structure's deterioration to mechanical properties. At present, there is no uniform division of rock pore size distribution, and there are different classification standards for rock samples in different areas. According to the characteristics of pore size distribution of red sandstone selected in this paper, the pore size distribution of red sandstone is divided into three categories: micropore (<3 nm), mesopore (3-50 nm), and macropore (≥50 nm). Table 2 shows the T_2 spectral area and small and medium pore area

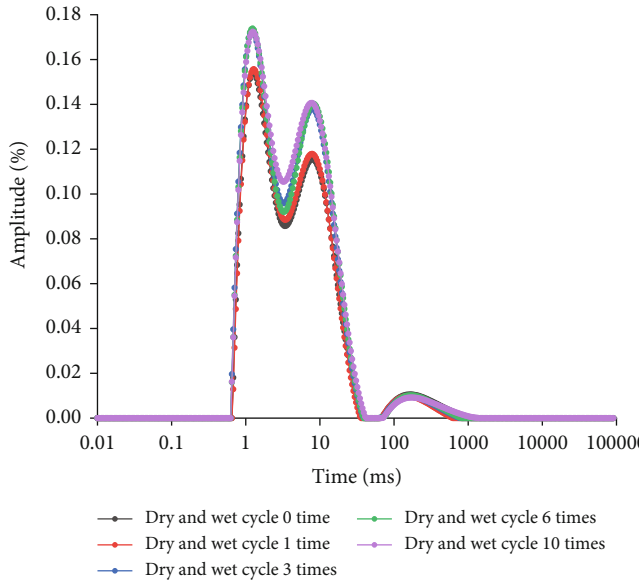

Figure 2: T_2 NMR spectrum of typical samples.

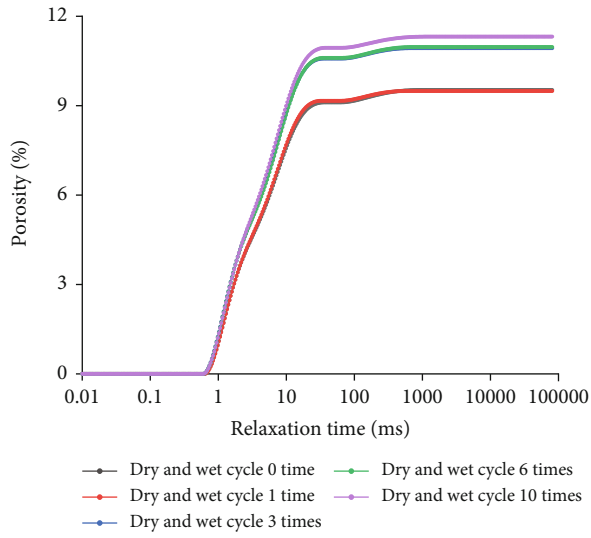

Figure 3: Cumulative porosity and relaxation time curve of red sandstone.

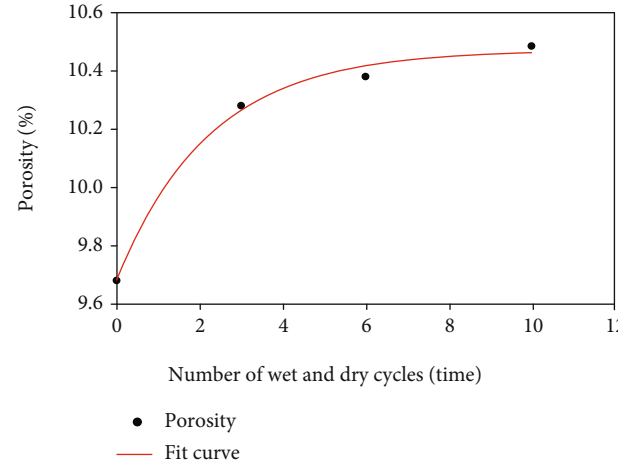

Figure 4: Fitting curve of relationship between porosity and number of dry and wet cycles.

Table 1: Changes of porosity after wet and dry cycle.

Number/time	0	1	3	6	10
Porosity/%	9.527	9.490	10.930	10.968	11.317
	9.841	9.437	9.627	9.787	9.646
Average	9.684	9.464	10.279	10.378	10.482

of red sandstone after different cycles of wet and dry. It can be seen from the table that the spectral area of red sandstone decreases by 1.301 after 0-1 cycle; 1-3 cycles increase by 0.622; the growth rate was 0.345 for 3-10 cycles, and the growth rate gradually decreased.

Figure 5 shows the data and fitting curve of the T_2 spectral area and the number of dry and wet cycles. The fitting results can be expressed in Formula (2), and the correlation coefficient $R^2 = 0.94834$, indicating that the spectral area S has a good exponential relationship with the number of dry and wet cycles N.

$$S = 6.3508 - 1.7455e^{(-N/1.9260)}, \quad (2)$$

where S is the spectral area, and N is the number of dry and wet cycles.

As can be seen from Figure 5 and Table 2, the total area of T_2 spectrum increases with the increase of the number of wet and dry cycles. During the 1-3 dry and wet cycles, the curve increases rapidly, indicating that the spectral area increases significantly. The internal pores develop rapidly under the

Table 2: T_2 spectral areas of red sandstone after different wet and dry cycles.

Cycle-index rock-sample	T_2 total spectrum area					T_2 spectrum small to medium pore area					T_2 spectrum macropore area				
	0	1	3	6	10	0	1	3	6	10	0	1	3	6	10
1	6.538	5.676	5.927	6.409	5.389	2.185	2.152	2.264	2.203	2.734	4.353	3.524	3.664	4.206	4.514
2	6.704	4.963	5.957	6.306	7.185	2.194	2.141	2.597	2.634	2.177	4.509	2.822	3.358	3.672	3.148
Average	6.621	5.320	5.942	6.358	6.287	2.190	2.147	2.431	2.419	2.456	4.431	3.173	3.511	3.939	3.831
Proportion/%						33.077	40.357	40.912	38.047	39.065	66.923	59.643	59.088	61.953	60.935

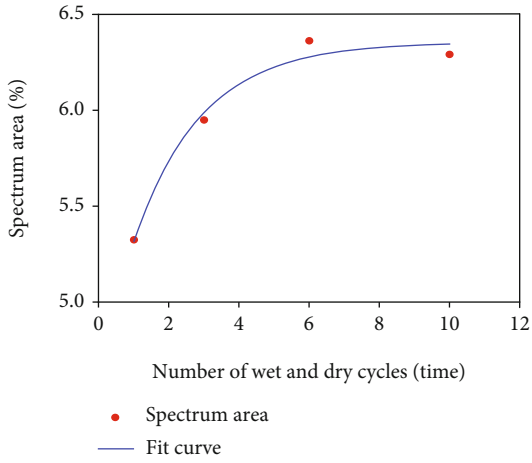

Figure 5: Fitting curve of relationship between the area of T_2 spectrum and the number of dry and wet cycles.

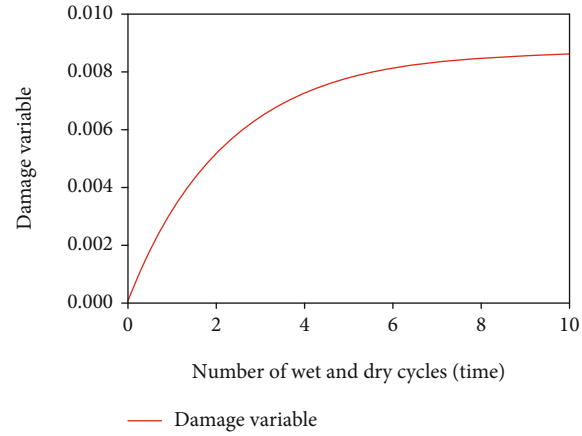

Figure 6: Variation curves of wet and dry cycles and damage degree.

action of the dry and wet cycles, especially the small and medium pores, which increase from 33.077% to 40.912%, with an increment of 7.835%. With the increase of the number of times, the growth rate of the curve slows down, the growth rate decreases, and the proportion of small and medium pores in the rock decreased, indicating that the growth rate of spectral area gradually slows down, fractures develop in the rock, and the expansion rate slows down. At this time, the proportion of small and medium pores in the rock decreases from 40.912% to 39.065%, with a decrement of 1.847%. Meanwhile, macropores increase from 59.088% to 60.935%, with an increment of 1.847%. The vast majority of small and medium pores in the rock expand into large pores, indicating that the dry-wet cycle has a certain influence on the development and connection of rock fractures. With the increase of cycle times, the curve finally tends to be stable, indicating that the development and expansion of pores in the rock caused by the dry-wet cycle has tended to be stable.

5. Damage Analysis of Dry and Wet Circulation

5.1. Damage Degree. Damage is the mechanical law of material property change and deformation failure caused by the irreversible deterioration process of fine microstructure and is an irreversible process in which the internal pore structure develops and expands continuously under the action of the dry and wet cycle.

In this paper, according to Song et al. [26], the continuous degree Ψ can be defined as follows:

$$\Psi = \frac{\tilde{V}}{V} = \frac{V_0(1-\mathrm{n})}{V_0(1-n_0)} = \frac{1-n}{1-n_0}, \tag{3}$$

$$V = V_0(1-n_0), \tag{4}$$

$$\tilde{V} = V_0(1-n), \tag{5}$$

where V is for damage in rock before a particle of volume, $\tilde{V}$ is for rock grain size after injury. n_0 is the initial porosity of all rock samples measured after natural water absorption and saturation for 48 h before the dry-wet cycle, and n is the porosity of rock samples measured after the dry-wet cycle. Since the dry-wet cycle has little influence on the total volume V_0 of rock samples, it is assumed that the total volume V_0 of rock samples remains unchanged before and after the dry-wet cycle.

According to Rabotnov [27], the damage variable D can be defined as follows:

$$D = 1 - \Psi. \tag{6}$$

When $D = 0$, it is the initial state, that is, lossless state, and when $D = 1$, it is the complete damage state.

Combination Formula (3)–(6), D can be expressed as follows:

$$D = 1 - \frac{\tilde{V}}{V} = 1 - \frac{1-n}{1-n_0} = \frac{n-n_0}{1-n_0}. \tag{7}$$

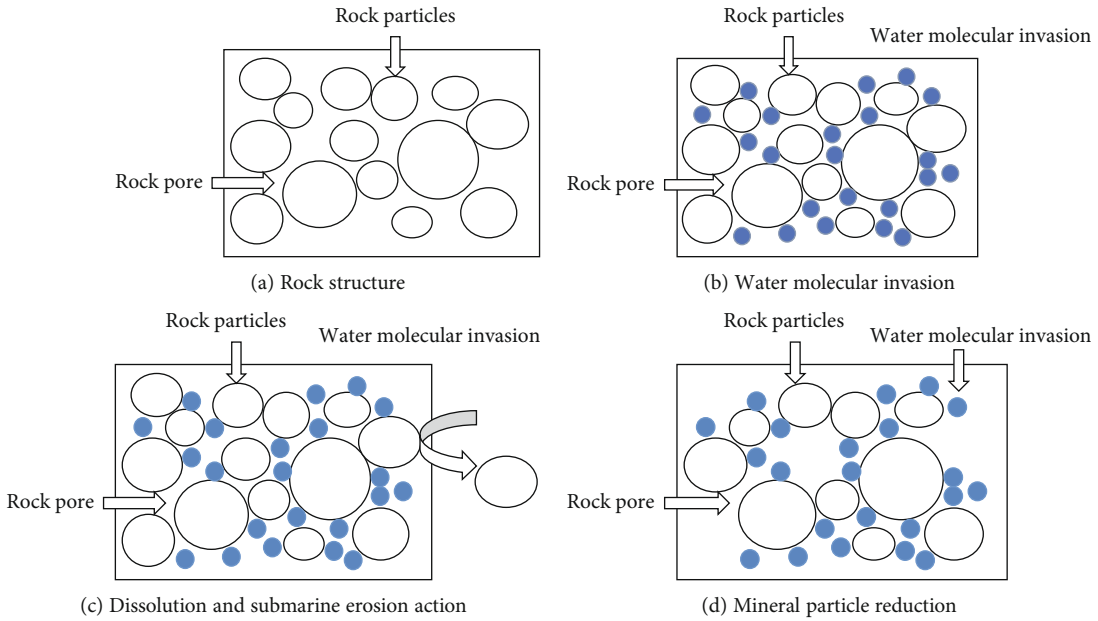

Figure 7: Failure mechanism diagram.

Equation (7) is the relationship between the porosity of rock samples and damage variables after the dry-wet cycle.

The initial porosity of the sample n_0 is 9.684%. By substituting the initial porosity and Formula (1) into the formula, the following equation can be obtained:

$$D = \frac{0.7860 - 0.7825e^{(-N/2.2424)}}{90.316}. \quad (8)$$

Equation (8) is the relationship between cycle number N and damage variable D under different dry and wet cycling conditions.

It can be seen from Figure 6 that when the number of dry and wet cycles is low, the curve rises faster and grows at a higher rate. The results show that the dry-wet cycle causes the pore structure in the rock to develop and expand rapidly, and the dry-wet cycle has an obvious damage effect on the red sandstone. When the frequency is large, the curve flattens out and the growth rate decreases, indicating that the dry-wet cycle has little influence on the internal pore structure of red sandstone and the damage degree decreases. With the continuous increase of the number of times, the damage degree tends to be fixed gradually because of the complete development and expansion of the internal pore structure.

5.2. Failure Mechanism. The failure mechanism of red sandstone in a neutral water environment can be summarized by combining the parameters of the meso-structure evolution process and the macroscopic expression of the sample. The influence of water on red sandstone is mainly reflected in the lubrication (soluble salt, hydrolytic colloid, the original connection into water glue connection, leading to the weakening of mineral particle connection force and friction, water plays the role of lubricant), water wedge action (when two mineral particles are close together and water molecules are added to the mineral surface, the mineral particles use their surface suction force to gather the water molecules around them and force the water molecules into the gap between the two mineral particles), pore pressure (reduces the compressive stress between particles, leaving the ends of the micro-fractures in the rock in a tensile state and thus breaking the rock connections), dissolution, and submersion (the permeable water in the rock can dissolve and take away the soluble material in the rock during its flow and sometimes wash away the small and medium particles of the rock, greatly reducing the strength and increasing the deformation of the rock).

Water molecules will permeate between mineral particles along the original pores and fissures in the rock. At this time, the primary pores become the main part of the physical and chemical reaction of water molecules. Water acts as a natural lubricant between mineral particles and weakens the connection between mineral particles. On this basis, soluble minerals and cementing materials contained in red sandstone are dissolved in water in the form of ions; the movement of water molecules is used as the internal driving force to move mineral ions out of the interior; and under the action of water wedge and pore pressure, large primary pores and secondary fractures are finally formed. After several dry and wet cycles, a large number of secondary fractures occur, which fundamentally change the overall structure of red sandstone and provide space conditions for corrosion and dissolution in the later period. The damage mechanism is shown in Figure 7.

6. Conclusion

(1) The T_2 spectrum curve is continuous and smooth, with three different peak spectra. Small and medium pores in red sandstone account for the majority, while large pores account for the least. With the increase of the number of dry and wet cycles, the

number of small and medium pores in red sandstone gradually increases, but the growth rate decreases. After 0-1 cycle, the spectral area of red sandstone decreases by 1.301; 1-3 cycles increase by 0.622; 3-10 cycles increase by 0.345. The spectral area increases with the increase of the number of wet and dry cycles, but the growth rate decreases and finally tends to be stable

(2) With the increase of the number of dry and wet cycles, the soluble material inside the rock is gradually dissolved under the action of water and produces new small pores. With the aggravation of damage, small and medium pores constantly develop and expand into large pores, resulting in an increasing number of internal pores and fractures. But eventually, the internal structure of the red sandstone will stabilize

(3) The functional relationship between the damage degree and the number of dry and wet cycles was established. When the number of wet and dry cycles is less than 6 times, the curve rises rapidly and grows rapidly. However, when the frequency is greater than 6, the curve tends to be flat, the growth rate decreases, the damage decreases significantly, and finally tends to be stable

(4) The damage of the dry-wet cycle to sandstone is mainly reflected in the physical damage of rock under the action of hydrostatic solution. Water enters the mineral particles along the cracks inside the rock, weakens the connection, and results in dissolution

Data Availability

The data used to support the findings of this study are included within the article.

Conflicts of Interest

The authors declare that they have no conflicts of interest.

References

[1] P. G. Zhou, "Engineering geomechanics study on the interaction between groundwater and geotechnical medium," *Study Leading Edge*, vol. 2, p. 176, 1996.

[2] H. Lin, S. J. Xie, R. Yong, Y. Chen, and S. du, "An empirical statistical constitutive relationship for rock joint shearing considering scale effect," *Comptes Rendus Mécanique*, vol. 347, no. 8, pp. 561–575, 2019.

[3] H. Lin, H. T. Yang, Y. X. Wang, Y. Zhao, and R. Cao, "Determination of the stress field and crack initiation angle of an open flaw tip under uniaxial compression," *Theoretical and Applied Fracture Mechanics*, vol. 104, article 102358, 2019.

[4] S. J. Xie, H. Lin, Y. F. Chen, R. Yong, W. Xiong, and S. Du, "A damage constitutive model for shear behavior of joints based on determination of the yield point," *International Journal of Rock Mechanics and Mining sciences*, vol. 128, p. 104269, 2020.

[5] X. X. Chen, H. L. Fu, and Q. Zhe, "Analysis of rock damage energy evolution of open pit slope under the action of wet and dry cycle," *Science Technology and Engineering*, vol. 16, no. 20, pp. 247–252, 2016.

[6] Y. Fu, X. R. Liu, and Y. X. Zhang, "Study on the influence of water-rock interaction on uniaxial strength of sandstone," *Hydrogeology and Engineering Geology*, vol. 36, no. 6, pp. 54–58, 2009.

[7] Y. L. Zhao, Y. X. Wang, and W. J. Wang, "Modeling of rheological fracture behavior of rock cracks subjected to hydraulic pressure and far field stresses," *Theoretical and Applied Fracture Mechanics*, vol. 101, pp. 59–66, 2019.

[8] Y. L. Zhao, L. Y. Zhang, and W. J. Wang, "Separation of elastoviscoplastic strains of rock and a nonlinear creep model," *International Journal of Geomechanics*, vol. 18, no. 1, article 04017129, 2018.

[9] Y. L. Zhao, L. Y. Zhang, and W. J. Wang, "Transient pulse test and morphological analysis of single rock fractures," *International Journal of Rock Mechanics & Mining Sciences*, vol. 91, pp. 139–154, 2017.

[10] Y. L. Zhao, L. Y. Zhang, and W. J. Wang, "Cracking and stress-strain behavior of rock-like material containing two flaws under uniaxial compression," *Rock Mechanics and Rock Engineering*, vol. 49, no. 7, pp. 2665–2687, 2016.

[11] T. L. Han, J. P. Shi, and Y. S. Chen, "Chemical corrosion and dry-wet circulation under the action of sandstone type I fracture toughness and strength parameters correlation research," *Journal of Hydraulic Engineering*, vol. 49, no. 10, pp. 1265–1275, 2018.

[12] K. G. Li, D. P. Zheng, and W. H. Huang, "Neural network simulation of mechanical properties and constitutive model of sandstone under dry-wet cycle," *Rock and Soil Mechanics*, vol. 34, no. S2, pp. 168–173, 2013.

[13] Z. L. Zhou, X. Cai, and Y. Zhao, "Strength characteristics of dry and saturated rock at different strain rates," *Transactions of Nonferrous Metals Society of China*, vol. 26, no. 7, pp. 1919–1925, 2016.

[14] Y. X. Wang, H. Zhang, and H. Lin, "Fracture behaviour of central-flawed rock plate under uniaxial compression," *Theoretical and Applied Fracture Mechanics*, vol. 106, article 102503, 2020.

[15] Y. X. Wang, P. P. Guo, W. X. Ren et al., "Laboratory investigation on strength characteristics of expansive soil treated with jute fiber reinforcement," *International Journal of Geomechanics*, vol. 17, no. 11, article 04017101, 2017.

[16] Y. Wang, H. Lin, and Y. Zhao, "Analysis of fracturing characteristics of unconfined rock plate under edge-on impact loading," *European Journal of Environmental and Civil Engineering*, vol. 24, pp. 2453–2468, 2019.

[17] H. Y. Li, "Analysis of pore structure of tight sandstone by nitrogen adsorption method," *Yunnan Chemical Technology*, vol. 46, no. 12, pp. 87–90, 2019.

[18] Z. C. Yan, C. S. Chen, and P. X. Fan, "Pore structure characterization of ten typical rocks in China," *Electronic Journal of Geotechnical Engineering*, vol. 20, no. 2, pp. 479–494, 2015.

[19] G. P. Frosch, J. E. Tillich, and R. Haselmeier, "Probing the pore space of geothermal reservoir sandstones by nuclear magnetic resonance," *Geothermics*, vol. 29, no. 6, pp. 671–687, 2000.

[20] K. P. Zhou, J. L. Li, and Y. J. Xu, "Determination of pore structure characteristics of rock based on nuclear magnetic resonance techniqueJournal of Central South University (Natural Science edition)," vol. 43, no. 12, pp. 4796–4800, 2012.

[21] J. L. Li, K. P. Zhou, and B. Ke, "Correlation analysis between pore development characteristics and uniaxial compressive strength of granite after freezing-thawing," *Journal of Coal*, vol. 40, no. 8, pp. 1783–1789, 2015.

[22] Z. G. Sun, D. Y. Jiang, and L. Li, "Study on thermal damage of Beishan granite based on low-field magnetic resonance," *Journal of Coal*, vol. 45, no. 3, pp. 1081–1088, 2020.

[23] S. Ren, X. S. Wang, and X. Ouyang, "Experimental study on fatigue damage of sandstone based on NMR and acoustic emission," *Journal of Beijing Institute of Technology*, vol. 39, no. 8, pp. 792–799, 2019.

[24] F. Pan, *Study on Landslide Hazard Assessment in Chuxiong City*, Southwest University of Science and Technology, 2018.

[25] Y. Z. Zhang and L. L. Xiao, "Experimental study on characteristics of rock nuclear magnetic resonance under uniaxial load," *Nuclear Electronics and Detection Technology*, vol. 6, pp. 731–734, 2006.

[26] Y. J. Song, L. T. Zhang, and J. X. Ren, "Research on dry-wet cycle damage characteristics of weakly consolidated sandstone based on nuclear magnetic resonance technology," *Journal of Rock Mechanics and Engineering*, vol. 38, no. 4, pp. 825–831, 2019.

[27] Y. N. Rabotnov, "On the equation of state of creep," in *ARCHIVE: Proceedings of the Institution of Mechanical Engineers, Conference Proceedings, 1964-1970, Various titles labelled Volumes A to S*, vol. 178, pp. 117–122, England, 1963.